

## Peristaltic Mixing of Bingham Fluids in a Closed Cavity: A Numerical Study

Zahra Poursharifi and Kayvan Sadeghy

Centre of Excellence in Design and Optimization of Energy Systems (CEDOES),  
School of Mechanical Engineering, College of Engineering, University of Tehran  
P.O. Box: 11155-4563, Tehran, Iran

### ABSTRACT

The effect of fluid's yield stress on the peristaltic mixing performance is investigated. Flow domain is a rectangular cavity with bottom wall generating a peristaltic wave. It is found that for small amplitude waves, yield stress improves the mixing performance. For large amplitude waves, yield stress weakens the mixing efficiency.

### INTRODUCTION

Peristaltic motion is an efficient means for fluid transport in physiological systems. It is also the basis of peristaltic pumps used in industry for the transport of slurries and highly viscous fluids. In recent years, it is increasingly being used as an efficient tool for mixing enhancement in microsystem devices. The need for mixing small volumes of fluid without the contact of any mechanical component in miniaturized devices has highlighted the efficiency of peristaltic mixers. In the past years, several investigations have been carried out to study the applicability of peristalsis for fluid handling in MEMS devices in several test cases<sup>1-3</sup>. In the theoretical domain, Yi et al.<sup>4</sup> was among the first who determined analytical solutions for this problem who derived the analytical profiles of velocity for small amplitude waves. In a similar study,

Selverov and Stone<sup>5</sup> developed theories for peristaltic transport in the rectangular cavity with one vibrating wall. Kumar et al.<sup>6</sup> numerically simulated the species transport, flow field and mixing in a peristaltically driven closed channel with one vibrating wall. Ng and Ma<sup>7</sup> investigated the steady Lagrangian flow field induced by small amplitude peristaltic waves applied to the walls of a closed cavity. As mentioned, a large amount of work has been carried out on the behavior of Newtonian fluids in peristaltic mixers and what has not been provided is the non-Newtonian fluids behavior in this regard. Considering the fact that a wide variety of physiological and industrial fluids fall in the category of viscoplastic fluids, we decide to study the Bingham fluid behavior in a peristaltic mixer addressing the effect of yield stress on the flow kinematics.

### MATHEMATICAL FORMULATION

We consider peristaltic flow of a Bingham fluid in a closed cavity of length  $L$  and height  $H$  (where  $A = L/H$  is the aspect ratio of channel) with a width much larger than the other two dimensions (see Fig. 1), so the flow induced in the channel can safely be taken as two-dimensional. The bottom wall is flexible whereas the three other walls are assumed to be rigid. As can

be seen in Fig. 1, a travelling wave is propagating from left to right giving rise to fluid transport in the streamwise direction.

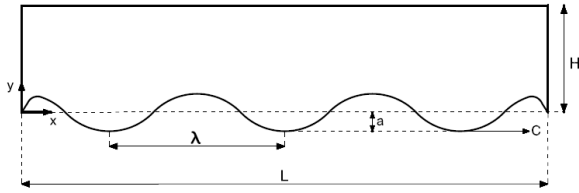


Figure 1. Schematic showing of the flow geometry.

The vibration mode of the bottom wall is followed by the model presented by Yi et al.<sup>4</sup> The peristaltic wave with the wavelength of  $\lambda$  and wave amplitude of  $\varepsilon H (= a)$  is applied to bottom wall of the domain while the side and top walls are fixed. Form of travelling wave for the bottom wall is generally written as:

$$y = \varepsilon H f(x, t, \omega, \lambda) \quad (1)$$

Where  $\omega$ ,  $\varepsilon$  and  $f$  represent the wave angular frequency, wave amplitude ratio and the wave shape, respectively.  $x$ ,  $y$  are the coordinates of a point on the wall and  $t$  is the time. Yi et al.<sup>4</sup> proposed the following expression for the wave shape function:

$$f(x, t) = \text{Re} \left\{ \exp \left( i \frac{2\pi}{\lambda} (x - ct) \right) \cdot \left( 1 - \exp \left( -\frac{x}{mH} \right) \cdot \left( 1 - \exp \left( \frac{x-L}{mH} \right) \right) \right) \right\} \quad (2)$$

The parameter  $m$  represents the stiffness of the bond that fixes the vibrating walls to the side walls. Incompressible fluid flow is governed by the general Cauchy equations accompanied with the continuity equation:

$$\frac{\partial \rho}{\partial t} + \nabla \cdot (\rho \mathbf{u}) = 0 \quad (3)$$

$$\rho \left( \frac{\partial \mathbf{u}}{\partial t} + \mathbf{u} \cdot \nabla \mathbf{u} \right) = -\nabla p + \nabla \cdot \boldsymbol{\tau} \quad (4)$$

For the sake of the current research where the fluid is assumed to be viscoplastic, we choose the Bingham model and rely on the bi-viscosity model defined as<sup>8</sup>:

$$\boldsymbol{\tau}_{ij} = \begin{cases} 2 \left( \mu_{\infty} + \frac{\tau_y}{\dot{\gamma}} \right) \mathbf{d}_{ij} & ; \text{ for } \dot{\gamma} \geq \dot{\gamma}_c \\ 2\mu_0 \mathbf{d}_{ij} & ; \text{ for } \dot{\gamma} < \dot{\gamma}_c \end{cases} \quad (5)$$

Where  $\tau_y$  is the fluid's yield stress,  $\mu_0$  is the viscosity of the un-yielded region, and  $\mu_{\infty}$  is the viscosity of the yielded zone ( $\mu_0 \gg \mu_{\infty}$ ).  $\dot{\gamma}$  is the second invariant of the rate-of-deformation tensor with  $\dot{\gamma}_c = \tau_y / (\mu_0 - \mu_{\infty})$  being the critical shear rate. To work with dimensionless parameters, we substitute:  $x^* = x/H$ ,  $y^* = y/H$ ,  $t^* = t\omega$ . We scale the velocity components with  $\varepsilon H \omega$  and the stress terms with  $\varepsilon H^2 \omega^2$ . By so doing, we eventually end up with the dimensionless form of the governing equations<sup>9</sup> which include the Bingham number (Bn) and Womersley number (Wo) defined as:

$$\text{Bn} = \frac{\tau_y}{\mu_{\infty} / \rho H}, \text{Wo} = H \sqrt{\frac{\omega}{\nu_{\infty}}} \quad (6)$$

## NUMERICAL METHOD

In the present work we rely on the multiple-relaxation-time lattice Boltzmann method (MRT-LBM)<sup>10</sup> for numerically solving the governing equations. In the

present work, we rely on the D2Q9 model; the nine discrete velocities used in this model are given as <sup>10</sup>:

$$\mathbf{c}_i = \begin{cases} (0,0) & i=0 \\ (\cos\theta, \sin\theta), \theta = \frac{(i-1)\pi}{2} & i=1,2,3,4 \\ \sqrt{2}(\cos\theta, \sin\theta), \theta = \frac{(i-5)\pi}{2} + \frac{\pi}{4} & i=5,6,7,8 \end{cases} \quad (7)$$

The probability distribution function which specifies the probability of finding fluid particles moving in a specific direction is defined as:

$$f_i(\mathbf{x}, t) \equiv f(\mathbf{x}, \mathbf{c}_i, t) \quad (8)$$

This function is the time-evolution of the probability distribution function which is represented by the lattice Boltzmann equation (LBE) <sup>10</sup>:

$$f_\alpha(\mathbf{x} + \mathbf{c}_\alpha \delta t, t + \delta t) - f_\alpha(\mathbf{x}, t) = \mathbf{\Omega}_{\alpha i} (f_i(\mathbf{x}, t) - f_i^{\text{eq}}(\mathbf{x}, t)) \quad (9)$$

$\mathbf{\Omega}_{\alpha i}$  is the collision matrix, and  $f_i^{\text{eq}}$  is the equilibrium distribution function given by <sup>10</sup>:

$$f_i^{\text{eq}} = w_i \rho \left[ 1 + 3\mathbf{c}_i \cdot \mathbf{u} + \frac{9}{2}(\mathbf{c}_i \cdot \mathbf{u})^2 - \frac{3}{2}\mathbf{u}^2 \right] \quad (10)$$

Where we have:  $w_0 = 4/9$ ,  $w_{1,2,3,4} = 1/9$ , and  $w_{5,6,7,8} = 1/36$ . In the present work, like our previous work <sup>11</sup>, we have decided to rely on the multiple-relaxation-time (MRT) method for the collision matrix  $\mathbf{\Omega}$ . (Please refer to Ref. <sup>11</sup>) In LBM, the macroscopic variables are calculated as:

$$\rho = \sum_{i=0}^8 f_i(\mathbf{x}, t); \quad \rho \mathbf{u} = \sum_{i=0}^8 \mathbf{c}_i f_i(\mathbf{x}, t), \quad (11)$$

Where  $\rho$  and  $\mathbf{u}$  are now the macroscopic density and velocity, respectively. LBM is very convenient for simulating of non-Newtonian fluids such as Bingham. This is mainly (unlike conventional numerical methods) the rate-of-deformation tensor ( $d_{ij}$ ) can be computed at each grid point with no need for the velocity gradient. This tensor can be locally determined at each grid point as <sup>11</sup>:

$$d_{ij} = -\frac{1}{2\rho c_s^2 \xi} \sum_{\alpha} \mathbf{c}_{\alpha i} \mathbf{c}_{\alpha j} \begin{pmatrix} f_{\alpha}(\mathbf{x}, t) \\ -f_{\alpha}^{\text{eq}}(\mathbf{x}, t) \end{pmatrix} \quad (12)$$

Where  $c_s = c/\sqrt{3}$  and  $\xi$  is the relaxation factor which is related to the kinematic viscosity by the relationship:  $\nu_{\infty} = (2\xi - 1)/6$ . As to satisfying the no-slip boundary condition at the fluid/solid interface, use can be made of the Ladd's bounce-back idea <sup>12</sup>. For the curved moving walls, we made use of an improved scheme of this rule by introducing parameter  $\Delta$  <sup>13</sup>:

$$\Delta = \frac{|\mathbf{x}_f - \mathbf{x}_w|}{|\mathbf{x}_f - \mathbf{x}_b|} \quad (13)$$

Where  $\mathbf{x}_f$  is the fluid node in the vicinity of the wall,  $\mathbf{x}_b$  is the solid node adjacent to the wall and  $\mathbf{x}_w$  is the intersection of the wall and the link connecting the fluid and solid node. Once  $\Delta$  is calculated, these steps should be followed <sup>13</sup>:

$$f_{\alpha}(x_w) = f_{\alpha}(x_f) + \Delta[f_{\alpha}(x_b) - f_{\alpha}(x_f)] + \Delta(\Delta - 1) \left( \frac{f_{\alpha}(x_b) - 2f_{\alpha}(x_f) + f_{\alpha}(x_f + \mathbf{e}_{\alpha}\delta t)}{2} \right) \quad (14)$$

$$f_{\bar{\alpha}}(x_w) = f_{\alpha}(x_w) + 2w_{\alpha} \rho_w \frac{3}{c^2} \mathbf{e}_{\alpha} \cdot \mathbf{u}_w. \quad (15)$$

$$f_{\bar{\alpha}}(x_f) = f_{\bar{\alpha}}(x_w) + \frac{\Delta}{1+\Delta} [f_{\bar{\alpha}}(x_f + \mathbf{e}_{\alpha}\delta t) - f_{\bar{\alpha}}(x_w)] - \left[ \frac{f_{\bar{\alpha}}(x_f + 2\mathbf{e}_{\alpha}\delta t)}{(2+\Delta)/\Delta} - \frac{f_{\bar{\alpha}}(x_f + \mathbf{e}_{\alpha}\delta t)}{(1+\Delta)/\Delta} + \frac{\Delta f_{\bar{\alpha}}(x_w)}{(2+\Delta)(1+\Delta)} \right] \quad (16)$$

In order to verify the numerical simulation, we compare our results with the analytical solution presented by Yi et al.<sup>4</sup> Fig. 2 depicts the comparison between the u-velocity profiles obtained from the numerical simulation in the middle cross section of channel (with one vibrating wall) and analytical solution for  $\varepsilon = 0.01$ ,  $k = 3.8$  ( $k$  is the dimensionless wave number),  $m = 0.02$ ,  $A = 5$  and  $Wo = 7.93$ . The comparison of the numerical results obtained in this study with the analytical solution shows a qualitative good agreement.

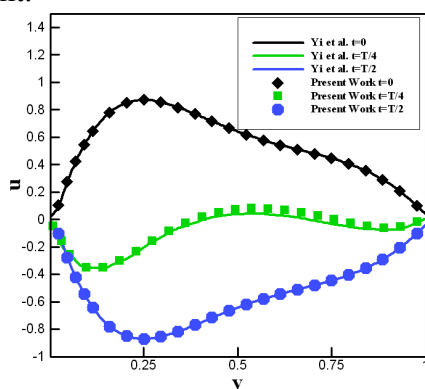


Figure 2. Comparison between our numerical results (symbols) with the analytical results (lines) reported in Ref. 4 for three different elapsed times.

RESULTS AND DISCUSSIONS

Having verified the numerical approach for the Newtonian fluid, we now present results addressing the effect of yield stress on the flow field (We show typical results only<sup>9</sup>). Fig. 3 and Fig. 4 depict the effect of Bingham number on the u-velocity profiles at the middle of the channel and along the horizontal centreline of the channel at two elapsed time steps for  $\varepsilon = 0.3$ ,  $k = 3.8$ ,  $m = 0.02$ ,  $A = 5$  and  $Wo = 7.93$ . These figures show that the yield stress has a significant effect on the velocity profiles. It is shown that for both cases, Bn effect has a non-trivial effect on the velocity profiles which seems to be related the location of the plugs.

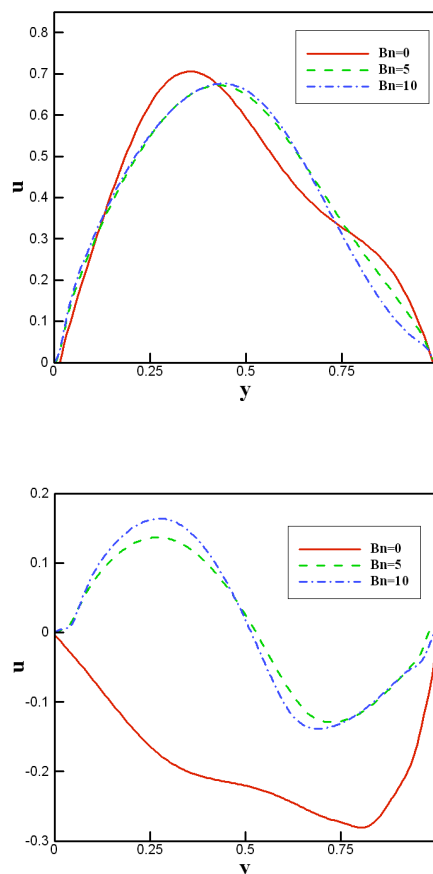


Figure 3. Effect of the Bingham number on the variation of the u-velocity profiles for  $x=L/2$ ;  $t=0$ (top),  $t=T/4$ (Bottom)

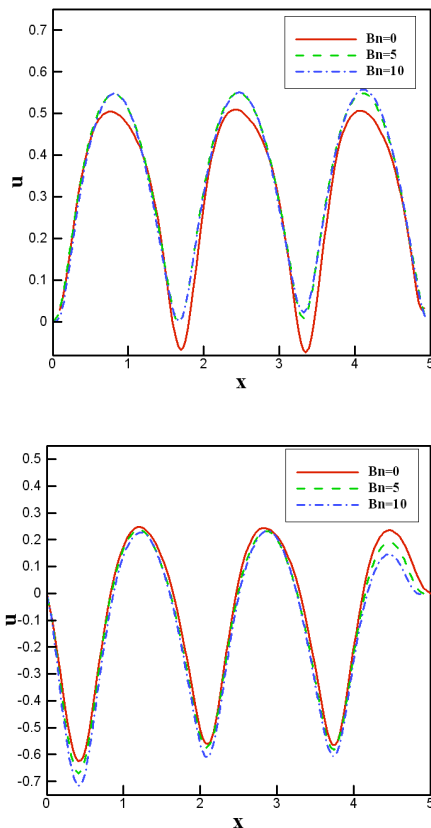


Figure 4. Effect of the Bingham number on the variation of the u-velocity profiles for  $y=0.5$ ;  $t=0$ (top),  $t=T/4$ (Bottom)

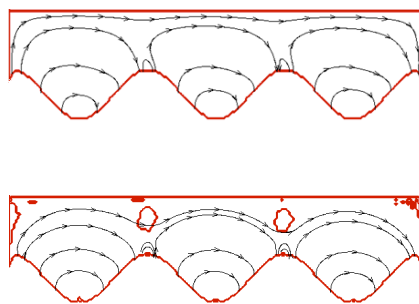


Figure 5. Effect of Bingham number on the streamline pattern;  $Bn=0$  (top),  $Bn=10$  (Bottom)

To further explore the effect of the Bingham number on peristaltic flow, in Fig. 5 we have shown its effect on the streamline pattern at the end of the cycle ( $t = T$ )

for  $m = 0.02$ ,  $A = 5$ ,  $k = 3.8$  and  $Wo = 7.93$ . It is shown that the sense of rotation of the secondary vortices is opposite to the primary ones. By increasing the Bingham number, the streamlines tend towards a more circular form.

In order to investigate the role played by the fluid's yield stress on the mixing efficiency. We have relied on the *drift parameter* as proposed by Ng and Ma<sup>7</sup>. It is a criterion based on the spatial-averaged value of the mass transport velocity. To this end we consider a set of Lagrangian particles introduced to the steady streaming flow and compare the mean drift transferred to them for different parameter values. The *mean drift parameter* is defined as<sup>7</sup>:

$$D_r = \frac{k}{2\pi} \int_0^1 \int_0^{2\pi/k} \sqrt{(\bar{u}_{lag}^2 + \bar{v}_{lag}^2)} dx dy \quad (17)$$

where  $\bar{u}_{lag}$  and  $\bar{v}_{lag}$  are the components of the mean Lagrangian velocity. Fig. 6 shows the effect of yield stress on the mean drift parameter for low deformation and high deformation waves for  $m = 0.02$ ,  $A = 5$ , and  $Wo = 7.93$ , respectively. As can be seen in these figures the mean drift parameter of Bingham fluids is larger than that of Newtonian fluids provided that the wave amplitude is smaller than a certain value. The situation becomes totally different when amplitude is large. As can be seen in Fig. 6 (bottom), at large amplitude, it is better for the fluid to have no yield stress as it decreases the mean drift of the flow.

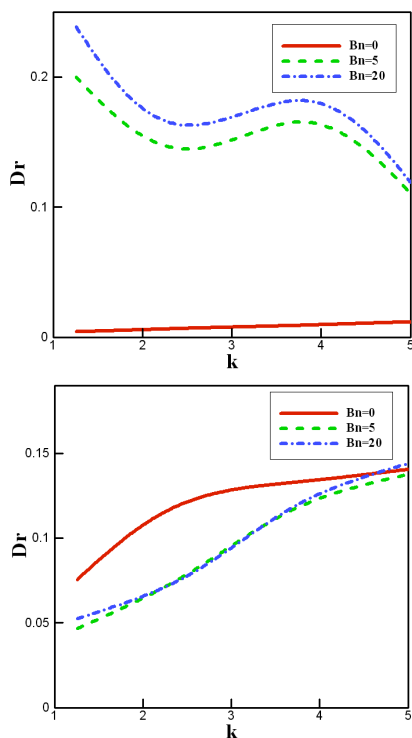


Figure 6. Effect of the Bingham number on the drift parameter obtained at different wave numbers:  $\varepsilon = 0.01$  (top),  $\varepsilon = 0.3$  (bottom)

### CONCLUDING REMARKS

In the present work, the effect of yield stress on the flow induced by peristaltic vibration of a single wall of a closed cavity is numerically investigated. The results indicate that the yield stress has a non-trivial effect on the variation of velocity profiles which is related to the plug morphology. Based on the results obtained for the mean drift parameter, one can conclude that the yield stress can improve the mixing performance of the flow field if the travelling wave is of small amplitude, while for the large-amplitude case, the yield stress has a negative effect on the mixing efficiency in the channel.

### REFERENCES

1. Bu, M., Melvin T., Ensell G., Wilkinson J.S., and Evans A.G.R. (2003), "Design and Theoretical Evaluation of a Novel Microfluidic Device to Be Used for PCR", *J. Micromech. Microeng.*, **13**, 125-130.
2. Xie, J., Shih, J., Lin, Q., Yang, B., and Taia, Y. (2004) "Surface Micromachined Electrostatically Actuated Micro Peristaltic Pump", *Lab Chip*, **4**, 495-501.
3. Sundararajan, N., Kim D., and Berlin, A.A. (2005) " Microfluidic Operations Using Deformable Polymer Membranes Fabricated by Single Layer Soft Lithography", *Lab Chip*, **5**, 350-354.
4. Yi, M., Bau, H. H., and Hu, H. (2002)" Peristaltically Induced Motion in a Closed Cavity with Two Vibrating Walls", *Phys. Fluids*, **14**, 184-197.
5. Selverov, K.P., and Stone, H.A. (2001) " Peristaltically Driven Channel Flows with Applications toward Micromixing", *Phys. Fluids*, **13**, 1837-1859.
6. Kumar, S., Kim, H.J., and Beskok, A. (2007) "Numerical Simulations of Peristaltic Mixing", *Journal of Fluids Engineering*, **129**, 1361-1371.
7. Ng, C., and Ma, Y. (2009) "Lagrangian Transport Induced by Peristaltic Pumping in a Closed Channel", *Physical Review E.*, **80**, 056307.
8. Beverly, C.R., and Tanner, R.I. (1992) " Numerical Analysis of Three-Dimensional Bingham Plastic Flow", *Journal of Non-Newtonian Fluid Mechanics*, **42**, 85-115.
9. Poursharifi, Z., PhD Thesis " Simulating Peristaltic Flow of Non-Newtonian Fluids in

Closed Cavity", University of Tehran, In progress.

10. Succi, S. (2001) "The Lattice Boltzmann Equation for Fluid Dynamics and Beyond", Oxford, Clarendon Press.

11. Khabazi, N.P., Taghavi, S.M., and Sadeghy, K. (2016) "Peristaltic Flow of Bingham Fluids at Large Reynolds Numbers: A Numerical Study", *Journal of Non-Newtonian Fluid Mechanics*, **227**, 30-44.

12. Ladd, A.J.C. (1994) "Numerical Simulation of Particular Suspensions via a Discretized Boltzmann Equation. Part 1. Theoretical Foundation", *J. Fluid. Mech.*, **271**, 285-309.

13. Yu, D., Mei, R., and Shyy, W. (2003) "A Unified Boundary Treatment in Lattice Boltzmann Method", *Proceedings of the 41st Aerospace Sciences Meeting and Exhibition, Reno, Nevada, 6-9 January AIAA*, 2003.